Nano-Hydroxyapatite Airborne-Particle Abrasion System as an Alternative Surface Treatment Method on Intraorally Contaminated Titanium Discs

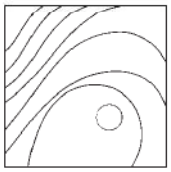

Kerem Çağlar Gümüş, DDS[1]
Gülbahar Ustaoğlu, DDS[1]
Levent Kara, PhD[2]*/Esra Ercan, DDS, PhD*[3]
Önder Albayrak, PhD[4]*/Mustafa Tunali, DDS, PhD*[3]

The aim of this study was to test the nano-hydroxyapatite powder decontamination method on intraorally contaminated titanium discs and to compare this method with current decontamination methods in the treatment of peri-implantitis. Contaminated discs were assigned to six treatment groups (n = 10 each): titanium hand curette; ultrasonic scaler with a plastic tip (appropriate for titanium); ultrasonic scaler with a plastic tip (appropriate for titanium) + H_2O_2; short-term airflow system (nano-hydroxyapatite airborne-particle abrasion for 30 seconds); long-term airflow system (nano-hydroxyapatite airborne-particle abrasion for 120 seconds); Er:YAG laser (120 mJ/pulse at 10 Hz). There were also two control groups (n = 10 each): contaminated disc (negative control) and sterile disc (positive control). Scanning electron microscopy, energy-dispersive x-ray spectroscopy, and dynamic contact angle analysis were used to determine the most effective surface-treatment method. The highest percentage of carbon (C) atoms was observed in the negative control group, and the lowest percentage of C atoms was found in the long-term airflow group, followed by the short-term airflow, laser, ultrasonic + H_2O_2, ultrasonic, and mechanical groups. When the groups were examined for wettability, the lowest contact angle degree was observed in the long-term airflow, short-term airflow, and laser groups. Nano-hydroxyapatite and laser treatments for detoxifying and improving infected titanium surfaces may show the most suitable results for reosseointegration.
Int J Periodontics Restorative Dent 2020;44:e179–e187. doi: 10.11607/prd.4852

[1]Department of Periodontology, Bolu Abant Izzet Baysal University, Bolu, Turkey.
[2]Department of Mechanical Engineering, Erzincan Binali Yıldırım University, Erzincan, Turkey.
[3]Department of Periodontology, Çanakkale Onsekiz Mart University, Çanakkale, Turkey.
[4]Department of Mechanical Engineering, Mersin University, Mersin, Turkey.

Correspondence to: Dr Gülbahar Ustaoğlu, Department of Periodontology, Faculty of Dentistry, Bolu Abant Izzet Baysal University, 14030, Bolu, Turkey. Fax: 0374 2546600. Email: gulbaharustaoglu@hotmail.com

Submitted January 31, 2020; accepted April 16, 2020.

Peri-implantitis is an inflammatory process that is characterized by bleeding, suppuration, and bone loss, and it affects the soft and hard tissues surrounding functioning implants.[1–3] There are some risk factors for development of peri-implantitis, such as poor oral hygiene, smoking, and history of periodontitis.[4] One or more of these factors lead to inflammation and degradation of the surface properties and biocompatibility of dental implants.[5] Although peri-implantitis and periodontitis have similar characteristics, they differ in some aspects,[6,7] and the treatment of these two diseases also varies. It is possible to restore the infected surface of the cementum in periodontal inflammation by cleaning and detoxifying the cementum with mechanical or chemical methods; however, detoxification of the implant surface is more challenging because of surface roughness. Biofilm removal alone is not sufficient for the reestablishment of the biocompatibility of titanium surfaces in implant surface treatment. Hydrophilic and biocompatible initial implant surface properties should be restored.

Different surface decontamination methods are often seen in the literature.[8–10] Decontamination techniques aim to eliminate calcified or bacterial deposits from the implant surface, restoring the implant appropriately for reosseointegration.[11,12]

Fig 1 *Acrylic appliance with five titanium discs attached.*

The methods used in the literature are mainly mechanical (involving the use of curettes made of metal, titanium, or carbon; ultrasonic scalers; or the use of an airborne-particle abrasion system) and chemical interventions (involving the use of chemicals, citric acid, chlorhexidine, and hydrogen peroxide), as well as laser treatments (including interventions with Er:YAG and Er,Cr:YSCG lasers).[13–15] Several studies have reported that airborne-particle abrasion systems and laser treatments may create an appropriate environment for reosseointegration rather than leading to changes on the implant surface.[16–18]

The major biologic step in the osseointegration phase of dental implants is cell adhesion at the interface between the host tissue and the implant. The anticipated structural and functional union of the implant with living bone is mostly influenced by the surface properties of the implant. The success of a dental implant depends on the chemical, physical, mechanical, and topographic characteristics of its surface. The influence of surface topography on osseointegration is associated with the duration of the healing processes.[19,20] A hydrophilic implant surface allows for better wettability and is manifested by the formation of a well-organized thrombus surrounding the implant. The wettability of the hard surfaces can be evaluated by measuring the contact angles and free surface energy.[21] The contact angle is defined as the angle of intersection of a line that is tangent to the liquid and a line tangent to the surface with the liquid. This angle demonstrates the characteristics of the substances in the implant system because the surface tension of the liquid and the surface energy of the solid structure can be modified by certain properties such as roughness. The wettability of the surface is increased with decreasing contact angles.[22,23]

The aim of the present study was to test the nano-hydroxyapatite (nano-HA) powder decontamination method on intraorally contaminated titanium discs and to compare this method with current decontamination methods in the treatment of peri-implantitis.

Materials and Methods

The protocol of the study was approved by the Bolu Abant Izzet Baysal University Clinical Research Ethics Committee (no: 2017/75). For in vivo biofilm formation, acrylic appliances (Essix C+ Plastic, Dentsply Sirona) containing five sterile, Grade 5 titanium discs (N = 70; SLA surface, OmniTech) with a 2-mm thickness and 10-mm diameter were used in the present study by 14 volunteers (7 men and 7 women). Volunteers were included in the study if they had good systemic health, no antibiotic treatment in the last 12 months, no signs of inflammation of periodontal tissues, no smoking, and a good level of oral hygiene. All participants gave written informed consent before the study-related procedures were carried out. The discs were placed in the appliances with their test surfaces facing the intraoral cavity and were applied to the palatal region (Fig 1). The volunteers used the appliances in their maxillae during a period of 48 hours. The appliances were not used during eating or drinking.[17] During this period, the teeth were not brushed with toothpaste, but mechanical cleaning was performed using water and a toothbrush. At the end of the 48-hour period, the discs were taken out of the appliances with care.

The contaminated discs were assigned to seven groups (n = 10 each; Table 1):

- Group 1: titanium hand curette for 120 seconds (Titanium IMP Scaler mini five 1/2, Hu-Friedy)
- Group 2: ultrasonic scaler with a polyether ether ketone (PEEK) fiber tip appropriate for titanium (Instrument PI, EMS) for 120 seconds
- Group 3: ultrasonic scaler with a PEEK fiber tip appropriate for titanium (Instrument PI) for 120 seconds + 3% H_2O_2 for 30 seconds
- Group 4: short-term airflow system (nano-HA airborne-particle abrasion; EMS Airflow S2, Hu-Friedy) for 30 seconds

Table 1 Comparison of Contact Angle Measurements by Group

Groups							
No.	Description	n	Mean	SD	Minimum	Maximum	*P*
1	Titanium hand curette	10	74.6250	11.10904	59.00	85.00	
2	Ultrasonic scaler with PEEK fiber tip	10	71.2222	4.94413	64.00	82.00	
3	Ultrasonic scaler with PEEK fiber tip + 3% H_2O_2	10	70.5000	5.42481	65.00	77.00	
4	Short-term airflow (30 s)	10	76.5556	5.41089	68.00	83.00	
5	Long-term airflow (120 s)	10	67.7778	5.76146	60.00	77.00	
6	Er:YAG laser (120 mJ/pulse at 10 Hz)	10	68.2500	7.59229	56.00	77.00	
7	Negative control (contaminated disc)	10	89.4000	9.44987	75.00	98.00	.005*
8	Positive control (sterile disc)	10	74.3750	3.54310	70.00	80.00	

SD = standard deviation; PEEK = polyether ether ketone.
Measurements are given in degrees.
*Statistically significant ($P < .05$).

- Group 5: long-term airflow system (nano-HA airborne-particle abrasion; EMS Airflow S2) for 120 seconds
- Group 6: Er:YAG laser (120 mJ/pulse at 10 Hz) for 120 seconds
- Group 7: contaminated disc (negative control)
- Group 8 (n = 10): sterile disc not used by any volunteers (positive control)

Instruments were applied by mimicking an intraoral approach with an approximately 30-degree angle. In the current study, commercially obtained nano-HA powders (calcium phosphate tribasic 34%–40% Ca, No. 36731, Alfa Aesar; Ca10(OH)2(PO4)6)) were used as the abrasive material. X-ray diffactrometry (XRD), Fourier transform infrared (FTIR), and scanning electron microscopy (SEM) analyses of these powders—performed in a previous study[24] by one of the authors—have proved that these nano-HA powders have a needle-like shape about 40 nm in width and 150 nm in length.

One investigator (K.G.) performed all treatment procedures in the same session to assure the reproducibility of the treatments. The negative control group and the processed test groups were examined under SEM. The investigator who performed the analysis (L.K.) was blinded to the treatment procedures.

SEM Analysis

The topographic analysis and chemical composition investigation of all specimens were performed using SEM (Quanta 450 FEG, FEI). Pretreatment SEM photos of the sterile titanium discs were taken to allow the comparison of before- and after-treatment differences on the surface of the discs. The discs were treated so that four groups of discs were prepared as follows: sterile titanium discs, erythrosine-stained titanium discs, biofilm-coated titanium discs, and biofilm-coated and erythrosine-stained titanium discs. After treating all samples, posttreatment SEM photographs of the samples were taken. The magnification powers used in the photographs were 50, 500, 1,000, and 2,000. The surface alterations were examined and compared. SEM images were evaluated in regard to similarity rate using MATLAB program (version R2017a, MathWorks) by histogram comparing method. As the "similarity" value approaches zero, the similarity between the compared visuals increases.

Energy-Dispersive X-Ray Spectroscopy Analysis

An energy-dispersive x-ray spectroscopy (EDS) analysis was performed for quantitative analysis of the titanium surfaces (Octane Plus, Quanta 450 FEG). From each group, three samples were examined to determine the chemical composition of the surface. Three different regions of each sample were examined. Spectroscopy of the emitted x-ray photons was performed with a Bruker detector with an energy resolution of approximately 123 eV at a working distance.

Dynamic Contact Angle Analysis

An Attension Theta Lite optical tensiometer (Biolin Scientific) equipped with an automatic drop deposition system, a high-speed video camera, and software were used to measure the advancing and receding contact angles (CAs) of the drops of distilled water. A Hamilton syringe with a volume of 1 mL was used to form liquid droplets. All CA values were reported with a standard deviation of ± 3 degrees. All measurements were conducted under normal atmospheric conditions and at room temperature. Hydrophilicity and CA hysteresis were examined by tensiometry using the Wilhelmy method by means of an electrobalance (Sigma 70, Biolin Scientific). The thermodynamic interrelations between the detected forces and CAs were noted. If the electrobalance detected different forces at the immersion and emersion times of the samples, the resulting difference in the advancing and receding CAs would be the CA hysteresis. The immersion velocity was set to 10 mm/minute for all experiments, and the immersion depth was 15 mm. All multiloop experiments were repeated at least four times at room temperature.

Statistical Analyses

Descriptive values of the data were calculated as means, standard deviations, minimums, and maximums. The homogeneity of the variance of the groups was examined by Levene test. When the variances were homogeneous, Kruskal-Wallis test was used to compare the groups. When variances were not homogeneous, Welch test was used to compare groups. The different groups were determined by nonparametric Dunn post hoc test or Games-Howel post hoc test. The statistical significance level was set at $P < .05$, and the SPSS program (version 25, IBM) was used for the calculations.

Results

SEM Analysis

In the mechanical treatment group, it was observed that the surface was flattened irregularly and contained crater-shaped halls.

In the laser treatment group, plaque elimination occurred as it did in the long-term airflow group. Minor changes, including small regions of flattening, were also observed in the laser treatment group.

Nano-HA particles were observed in the short- and long-term airflow groups. A rough surface structure closely resembled the original surface structure. The authors saw virtually no residual implant surface roughening material in the long-term airflow group.

In the negative control group, a biofilm layer developed and covered the surface of the titanium disc, hiding its rough surface structure.

In the ultrasonic and ultrasonic + H_2O_2 groups, wide and flat regions neighboring irregular groove-like craters were observed on the titanium surface. Some residual material was present in the center of the flat areas. It was assumed that the PEEK probe wore out and caused the presence of this material (Fig 2).

Comparison of SEM images in terms of similarity rate was calculated with the histogram method, and the best similarity rate was found in the laser treatment group (Table 2).

EDS Analysis

The EDS analysis results revealed that calcium and phosphorus ions in the short- and long-terms airflow groups were present in different amounts compared to that of the other groups. In the long-term group, there were more calcium and phosphorous ions than in the short-term group. The highest percentage of carbon atoms was observed in the negative control group, and the lowest percentage of carbon atoms was found in the airflow groups, followed by the laser, ultrasonic + H_2O_2, ultrasonic, and mechanical groups. The highest atomic percentages of titanium were present in the short- and long-term airflow groups. The atomic percentage of titanium was lower in the negative control group due to plaque formation. Oxygen levels were variable on the surfaces (Fig 3).

CA Measurement

As the CA degree increased, the wettability decreased proportionally. When the groups were examined for wettability, the lowest CA degrees were observed in the short-term airflow, long-term airflow, and laser groups (Table 1 and Fig 4).

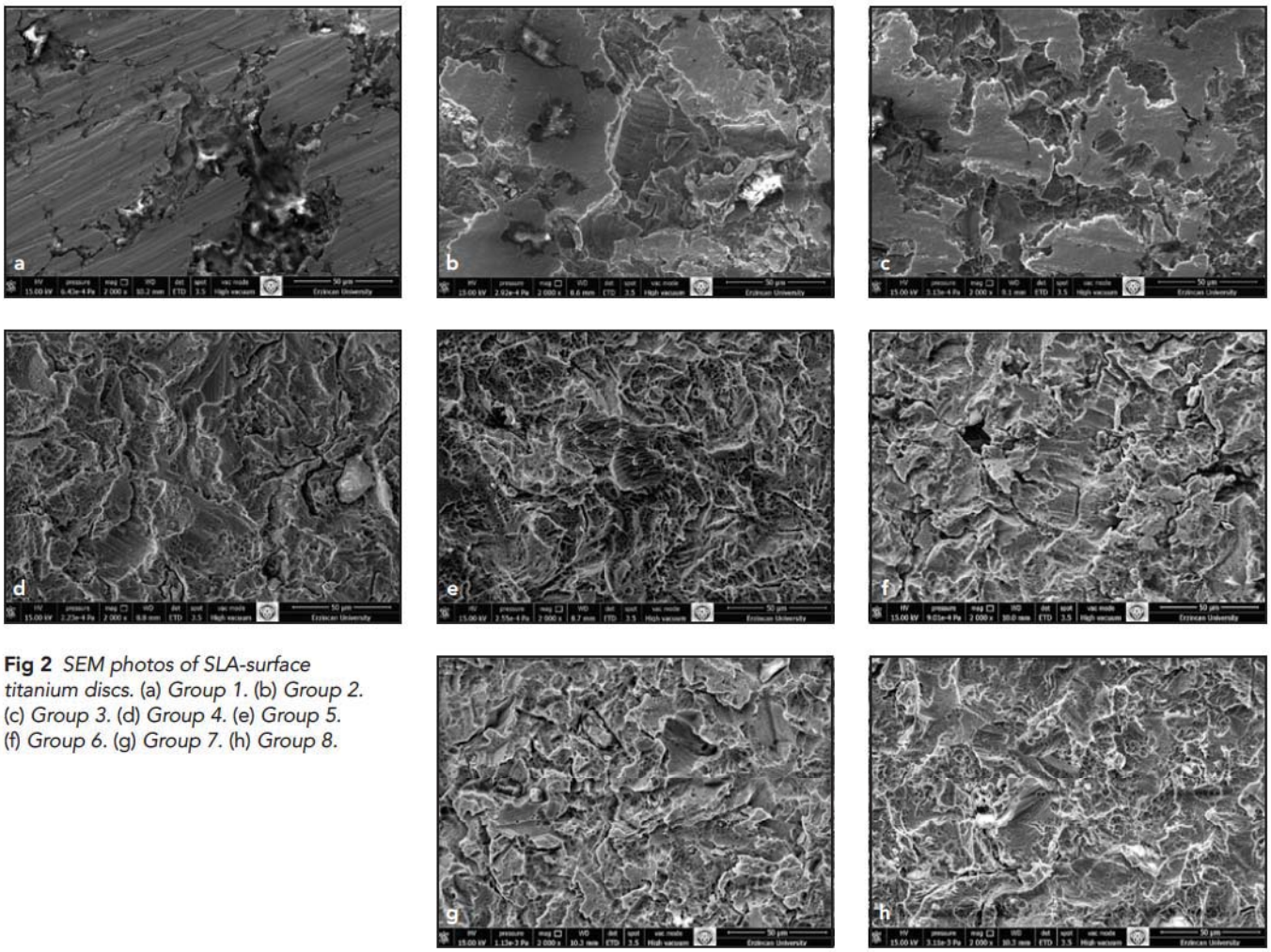

Fig 2 *SEM photos of SLA-surface titanium discs.* (a) *Group 1.* (b) *Group 2.* (c) *Group 3.* (d) *Group 4.* (e) *Group 5.* (f) *Group 6.* (g) *Group 7.* (h) *Group 8.*

Discussion

In the present study, the authors investigated the effects of different surface treatment methods on peri-implantitis by performing SEM and EDS analyses and measuring CAs. Although several studies are available in the literature that compare detoxification methods that use titanium discs,[17,25] to the best of the authors' knowledge, there are no studies that use SEM and EDS analyses of CA measurements. In the present study, the SEM images revealed flattening, deformation, and residual material on the titanium surfaces in the titanium curette, ultrasonic PEEK, and ultrasonic + H_2O_2 groups. In the airflow and laser groups, the rate of deformation on the rough surface was lower, and the structure of the surfaces resembled the original ones more closely. Nano-HA particles were seen in the short- and long-term airflow groups. The presence of nano-HA particles on the surface may provide an advantage in terms of reosseointegration, as nano-HA has specific properties, such as the ability to chemically bond to bone,

Table 2 Comparison of SEM Images: Similarity Rate by Histogram Method

Group	Mean similarity rate
1	0.003355
2	0.000994
3	0.001363
4	0.000517
5	0.000561
6	0.000258
7	0.002257
8	0

As the similarity value approaches 0, the similarity between the visuals compared increases.

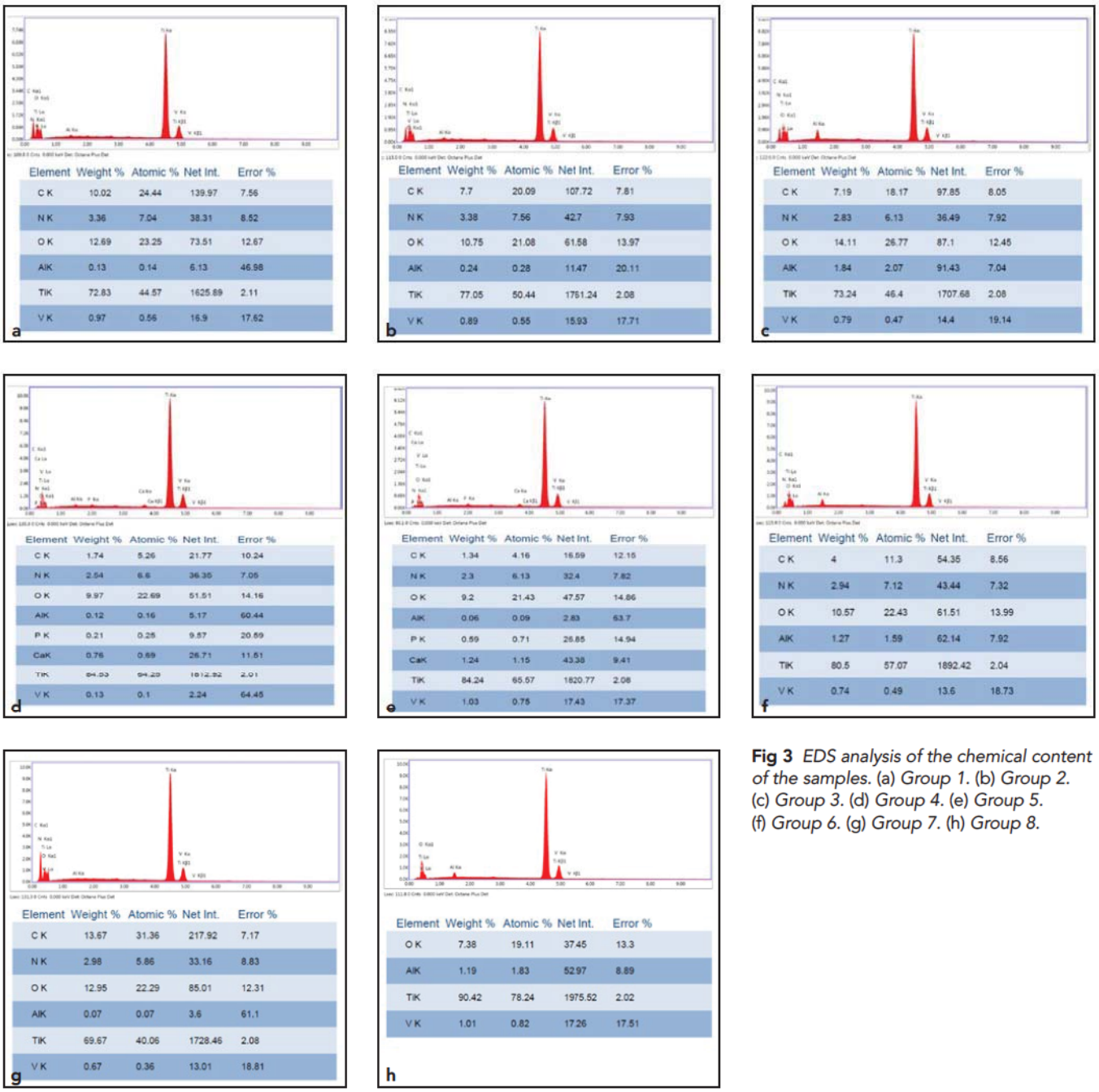

a

Element	Weight %	Atomic %	Net Int.	Error %
C K	10.02	24.44	139.97	7.56
N K	3.36	7.04	38.31	8.52
O K	12.69	23.25	73.51	12.67
Al K	0.13	0.14	6.13	46.98
Ti K	72.83	44.57	1625.89	2.11
V K	0.97	0.56	16.9	17.62

b

Element	Weight %	Atomic %	Net Int.	Error %
C K	7.7	20.09	107.72	7.81
N K	3.38	7.56	42.7	7.93
O K	10.75	21.08	61.58	13.97
Al K	0.24	0.28	11.47	20.11
Ti K	77.05	50.44	1751.24	2.08
V K	0.89	0.55	15.93	17.71

c

Element	Weight %	Atomic %	Net Int.	Error %
C K	7.19	18.17	97.85	8.05
N K	2.83	6.13	36.49	7.92
O K	14.11	26.77	87.1	12.45
Al K	1.84	2.07	91.43	7.04
Ti K	73.24	46.4	1707.68	2.08
V K	0.79	0.47	14.4	19.14

d

Element	Weight %	Atomic %	Net Int.	Error %
C K	1.74	5.26	21.77	10.24
N K	2.54	6.6	36.35	7.05
O K	9.97	22.69	51.51	14.16
Al K	0.12	0.16	5.17	60.44
P K	0.21	0.25	9.57	20.59
Ca K	0.76	0.69	26.71	11.51
Ti K	84.93	94.29	1812.52	2.01
V K	0.13	0.1	2.24	64.45

e

Element	Weight %	Atomic %	Net Int.	Error %
C K	1.34	4.16	16.59	12.15
N K	2.3	6.13	32.4	7.82
O K	9.2	21.43	47.57	14.86
Al K	0.06	0.09	2.83	53.7
P K	0.59	0.71	26.85	14.94
Ca K	1.24	1.15	43.38	9.41
Ti K	84.24	65.57	1820.77	2.08
V K	1.03	0.75	17.43	17.37

f

Element	Weight %	Atomic %	Net Int.	Error %
C K	4	11.3	54.35	8.56
N K	2.94	7.12	43.44	7.32
O K	10.57	22.43	61.51	13.99
Al K	1.27	1.59	62.14	7.92
Ti K	80.5	57.07	1892.42	2.04
V K	0.74	0.49	13.6	18.73

g

Element	Weight %	Atomic %	Net Int.	Error %
C K	13.67	31.36	217.92	7.17
N K	2.98	5.86	33.16	8.83
O K	12.95	22.29	85.01	12.31
Al K	0.07	0.07	3.6	61.1
Ti K	69.67	40.06	1728.46	2.08
V K	0.67	0.36	13.01	18.81

h

Element	Weight %	Atomic %	Net Int.	Error %
O K	7.38	19.11	37.45	13.3
Al K	1.19	1.83	52.97	8.89
Ti K	90.42	78.24	1975.52	2.02
V K	1.01	0.82	17.26	17.51

Fig 3 *EDS analysis of the chemical content of the samples.* (a) *Group 1.* (b) *Group 2.* (c) *Group 3.* (d) *Group 4.* (e) *Group 5.* (f) *Group 6.* (g) *Group 7.* (h) *Group 8.*

that do not cause any toxicity or inflammation. EDS analyses showed that all detoxification methods were effective in eliminating plaques. The most effective methods were found to be the airflow methods, followed by the laser, ultrasonic, ultrasonic + H_2O_2, and titanium curette methods.

In this study, carbon was observed in all study groups, but the lowest carbon ratio was observed in the long-term airflow group, without any use of carbon curettes. It is suggested that the carbon observed in the study originated from plaques.

In an in vitro study conducted by Tastepe et al,[17] EDS analysis revealed titanium ions at high rates in all study groups. In the control group, the EDS analysis revealed carbon, silicium, and sulphur. The authors associated this condition with the formation of saliva and bio-

Fig 4 *CA measurements for all groups.* (a) *Group 1.* (b) *Group 2.* (c) *Group 3.* (d) *Group 4.* (e) *Group 5.* (f) *Group 6.* (g) *Group 7.* (h) *Group 8.*

film, which was similar to the findings of the present study. Tastepe et al observed calcium and phosphorous ions in the HA group and HA + TCP airborne-particle abrasion group.[17]

Hydrophilicity is a major factor for the initial stabilization of a thrombus and the formation of fibrin induced by a healthy titanium structure around implants. This factor is why implant surfaces are required to be specifically clean and hydrophilic. Studies in the literature support this information.[26–28] A clean titanium surface will allow thrombocytes to be activated more efficiently, and it will allow the formation of fibrin to surround the implant in minutes. Gamal et al[29] used nano-HA and blood on peri-implantitis–affected surface conditioning with citric acid and saw improved clot adhesion to titanium implant surfaces. This study used nano-HA as clot-blended graft material.[29]

The present study demonstrated that, after decontamination, the hydroxyapatite long-term group developed the most effective hydrophilicity on the implant surfaces contaminated with plaque. The laser group developed a favorable degree of hydrophilicity on the surface as well.

Lee et al[9] also evaluated the CA of contaminated titanium surfaces after mechanical treatment alone or combined with chlorhexidine irrigation, as well as mechanical treatment combined with ultrasonication. Those authors found that both methods showed a high CA and low hydrophilicity and were insufficient to remove all bacterial products. Additionally, the authors concluded that residual bacterial products on implant surfaces may reduce hydrophilicity and further prevent the attachment of osteoblasts.

In their study on surface implants with peri-implantitis, Rosen et al[30] also found that mechanical decontamination methods were insufficient for reosseointegration, and they tried to develop a new protocol for decontamination of peri-implantitis surfaces.

In the present study, treatment with nano-HA in combination with a 2-minute-long airflow provided a much better hydrophilic surface compared to the 30-second-long airflow application. Therefore, the present authors are of the opinion that further studies should give importance to the method, duration, and mode of application of decontamination to remove all bacterial products as well as the reosseointegration of bone.

In a study by Tastepe et al, osteoconductive power (hydroxyapatite) powder was applied with an airborne-particle abrasion system.[31] These authors showed the cleaning effect of infected implant surfaces both in vitro and ex vivo. This method preserved the surface morphology, except for micro-hydroxyapatite particles embedded in titanium. This modified surface seemed to improve the osteoconductive properties because of buried HA particles. Additionally, remaining osteoconductive powder particles (hydroxyapatite and calcium phosphate) are supposed to create a modified implant surface and to stimulate bone growth towards the implant surface.[31] In another study that evaluated the disc surfaces roughened by hydroxyapatite but not by nano-HA, Tastepe et al observed the inadvertent formation of pointed edges, creating a more irregular surface structure.[17] Therefore, these authors used microparticles of hydroxyapatite (5 µm) to avoid any damage to the titanium surface. When the particles hit the surface, they crashed into small pieces and indwelled to deep grooves.

In the literature, some airborne-particle abrasion powders, such as amino acid glycine, erythritol, and glycine, have been used and were found to be more effective than mechanical treatment procedures in peri-implantitis treatment.[32–34] In the present study, the authors wanted to use a powder that included similar ingredients with bone. One of the aims of this study was to create a surface similar to bone. Bone consists of about 60% hydroxyapatite. The inorganic component of bone is made of the small plate-shaped hydroxyapatite crystals (20 to 50 nm long, 15 nm wide, and 2 to 5 nm thick).[35] So, after treatment, the residual nano-HA particles may mimic bone. Nano-HA was used in the present study, and the particles were observed on the surfaces of the tested specimens and enhanced wettability by creating a bioactive surface.

Meirelles et al[36] concluded that increased bone formation was found with the nano-HA–coated titanium implants compared to uncoated implants after 4 weeks of healing, according to histologic results. This study showed that early bone formation was dependent on the nano-HA, and these results support the hypothesis of the present study.[36]

Conclusions

This study had various limitations. Dental implant surfaces have different surface textures and screws, and this makes them difficult to clean. Additionally, surgical sites may be difficult to reach, which can complicate the cleaning of the titanium surface. Also, the test samples used were contaminated with supragingival plaque, which may show differences from plaque formation of peri-implant pocket. In vivo studies may be useful for shedding light on these methods.

Within the limitations of the study, it was found that the most appropriate methods for detoxifying and improving the surfaces of infected implants to become more suitable for clot adhesion and wound stabilization were airborne-particle abrasion systems (nano-HA powder) and laser treatments. However, the authors cannot claim that either method improved the surfaces to achieve a structure similar to that of the surface at the time of the implant. Further studies are required to investigate the renovation of the implant surface intraorally in harmony with and without harming the surrounding tissues. In addition, future clinical trials with Grade IV and Grade V dental implants will contribute to the clarification of the subject.

Acknowledgments

No competing financial interests exist.

References

1. Lindhe J, Meyle J, Group DoEWoP. Peri-implant diseases: Consensus report of the Sixth European Workshop on Periodontology. J Clin Periodontol 2008; 35(suppl 8):s282–s285.

2. Padial-Molina M, Suarez F, Rios HF, Galindo-Moreno P, Wang HL. Guidelines for the diagnosis and treatment of peri-implant diseases. Int J Periodontics Restorative Dent 2014;34:e102–e111.
3. Zitzmann NU, Berglundh T. Definition and prevalence of peri-implant diseases. J Clin Periodontol 2008;35 (suppl 8):s286–s291.
4. Berglundh T, Armitage G, Araújo MG, et al. Peri-implant diseases and conditions: Consensus report of Workgroup 4 of the 2017 World Workshop on the Classification of Periodontal and Peri-Implant Diseases and Conditions. J Periodontol 2018;89(suppl 1):s313–s318.
5. Trino LD, Bronze-Uhle ES, Ramachandran A, Lisboa-Filho PN, Mathew MT, George A. Titanium surface bio-functionalization using osteogenic peptides: Surface chemistry, biocompatibility, corrosion and tribocorrosion aspects. J Mech Behav Biomed Mater 2018;81:26–38.
6. Berglundh T, Zitzmann NU, Donati M. Are peri-implantitis lesions different from periodontitis lesions? J Clin Periodontol 2011;38(suppl 11):s188–s202.
7. Heitz-Mayfield LJ, Lang NP. Comparative biology of chronic and aggressive periodontitis vs. peri-implantitis. Periodontol 2000 2010;53:167–181.
8. Cao J, Wang T, Pu Y, Tang Z, Meng H. Influence on proliferation and adhesion of human gingival fibroblasts from different titanium surface decontamination treatments: An in vitro study. Arch Oral Biol 2018;87:204–210.
9. Lee BS, Shih KS, Lai CH, Takeuchi Y, Chen YW. Surface property alterations and osteoblast attachment to contaminated titanium surfaces after different surface treatments: An in vitro study. Clin Implant Dent Relat Res 2018; 20:583–591.
10. Hakki SS, Tatar G, Dundar N, Demiralp B. The effect of different cleaning methods on the surface and temperature of failed titanium implants: An in vitro study. Lasers Med Sci 2017;32:563–571.
11. Schwarz F, Rothamel D, Sculean A, Georg T, Scherbaum W, Becker J. Effects of an Er:YAG laser and the Vector ultrasonic system on the biocompatibility of titanium implants in cultures of human osteoblast-like cells. Clin Oral Implants Res 2003;14:784–792.
12. Mombelli A, Lang NP. Microbial aspects of implant dentistry. Periodontol 2000 1994;4:74–80.
13. Schwarz F, Sculean A, Rothamel D, Schwenzer K, Georg T, Becker J. Clinical evaluation of an Er:YAG laser for nonsurgical treatment of peri-implantitis: A pilot study. Clin Oral Implants Res 2005; 16:44–52.
14. Al-Hashedi AA, Laurenti M, Benhamou V, Tamimi F. Decontamination of titanium implants using physical methods. Clin Oral Implants Res 2017;28: 1013–1021.
15. Gosau M, Hahnel S, Schwarz F, Gerlach T, Reichert TE, Bürgers R. Effect of six different peri-implantitis disinfection methods on in vivo human oral biofilm. Clin Oral Implants Res 2010;21: 866–872.
16. Quintero DG, Taylor RB, Miller MB, Merchant KR, Pasieta SA. Air-abrasive disinfection of implant surfaces in a simulated model of peri-implantitis. Implant Dent 2017;26:423–428.
17. Tastepe CS, Liu Y, Visscher CM, Wismeijer D. Cleaning and modification of intraorally contaminated titanium discs with calcium phosphate powder abrasive treatment. Clin Oral Implants Res 2013;24:1238–1246.
18. Madi M, Htet M, Zakaria O, Alagl A, Kasugai S. Re-osseointegration of dental implants after peri-implantitis treatments: A systematic review. Implant Dent 2018;27:101–110.
19. Grassi S, Piattelli A, de Figueiredo LC, et al. Histologic evaluation of early human bone response to different implant surfaces. J Periodontol 2006;77:1736–1743.
20. Cochran DL, Buser D, ten Bruggenkate CM, et al. The use of reduced healing times on ITI implants with a sand-blasted and acid-etched (SLA) surface: Early results from clinical trials on ITI SLA implants. Clin Oral Implants Res 2002;13:144–153.
21. Tavana H, Neumann AW. Recent progress in the determination of solid surface tensions from contact angles. Adv Colloid Interface Sci 2007;132:1–32.
22. Winkler S, Ortman HR, Ryczek MT. Improving the retention of complete dentures. J Prosthet Dent 1975;34:11–15.
23. Ortman HR, Winkler S, Morris HF. Clinical and laboratory investigation of a ceramic-filled acrylic resin compound. J Prosthet Dent 1970;24:253–267.
24. Albayrak O, Ipekoglu M, Mahmutyazicioglu N, Varmis M, Kaya E, Altintas S. Preparation and characterization of porous hydroxyapatite pellets: Effects of calcination and sintering on the porous structure and mechanical properties. Proc Inst Mech Eng Pt L J Mater Des Appl 2016;230:985–993.
25. Charalampakis G, Ramberg P, Dahlén G, Berglundh T, Abrahamsson I. Effect of cleansing of biofilm formed on titanium discs. Clin Oral Implants Res 2015;26:931–936.
26. Donos N, Hamlet S, Lang NP, et al. Gene expression profile of osseointegration of a hydrophilic compared with a hydrophobic microrough implant surface. Clin Oral Implants Res 2011;22:365–372.
27. Lang NP, Salvi GE, Huynh-Ba G, Ivanovski S, Donos N, Bosshardt DD. Early osseointegration to hydrophilic and hydrophobic implant surfaces in humans. Clin Oral Implants Res 2011;22: 349–356.
28. Sartoretto SC, Calasans-Maia JA, da Costa YO, Louro RS, Granjeiro JM, Calasans-Maia MD. Accelerated healing period with hydrophilic implant placed in sheep tibia. Braz Dent J 2017;28: 559–565.
29. Gamal AY, Abdel-Ghaffar KA, Iacono VJ. A novel approach for enhanced nanoparticle-sized bone substitute adhesion to chemically treated peri-implantitis-affected implant surfaces: An in vitro proof-of-principle study. J Periodontol 2013;84:239–247.
30. Rosen PS, Qari M, Froum SJ, Dibart S, Chou LL. A pilot study on the efficacy of a treatment algorithm to detoxify dental implant surfaces affected by peri-implantitis. Int J Periodontics Restorative Dent 2018;38:261–267.
31. Tastepe CS, Lin X, Donnet M, Wismeijer D, Liu Y. Parameters that improve cleaning efficiency of subgingival air polishing on titanium implant surfaces: An in vitro study. J Periodontol 2017;88:407–414.
32. Renvert S, Lindahl C, Roos Jansaker AM, Persson GR. Treatment of peri-implantitis using an Er:YAG laser or an air-abrasive device: A randomized clinical trial. J Clin Periodontol 2011;38:65–73.
33. John G, Sahm N, Becker J, Schwarz F. Nonsurgical treatment of peri-implantitis using an air-abrasive device or mechanical debridement and local application of chlorhexidine. Twelve-month follow-up of a prospective, randomized, controlled clinical study. Clin Oral Investig 2015;19:1807–1814.
34. Toma S, Lasserre JF, Taïeb J, Brecx MC. Evaluation of an air-abrasive device with amino acid glycine-powder during surgical treatment of peri-implantitis. Quintessence Int 2014;45:209–219.
35. Feng X. Chemical and biochemical basis of cell-bone matrix interaction in health and disease. Curr Chem Biol 2009;3:189–196.
36. Meirelles L, Arvidsson A, Andersson M, Kjellin P, Albrektsson T, Wennerberg A. Nano hydroxyapatite structures influence early bone formation. J Biomed Mater Res A 2008;87:299–307.